Effect of tartaric acid and phosphoric acid on the water resistance of magnesium oxychloride (MOC) cements

Xiaoyang Chen[a], Tingting Zhang[b], Wanli Bi[a]*, Christopher Cheeseman[c]

[a]School of High-Temperature Materials and Magnesia Resources Engineering, University of Science and Technology, Liaoning, P.R.China

[b]Faculty of Infrastructure Engineering, Dalian University of Technology, Dalian, Liaoning, P.R. China

[c] Department of Civil and Environmental Engineering, Imperial College London, UK

*Corresponding author: Wanli Bi, E-mail: asbwl@126.com

ABSTRACT

Magnesium oxychloride (MOC) cements have high early strength, low thermal conductivity and low density, but are not used widely in construction because they have poor water resistance. This research has investigated the effects of phosphoric acid and tartaric acid additions on the water resistance of MOC cement pastes. The effect on setting time, hydration reactions, compressive strength, phase composition, thermal stability and microstructure are reported. Phosphoric acid and tartaric acid additions of 1wt.% significantly improve the water resistance of MOC cements pastes and this is associated with increased $5Mg(OH)_2 \cdot MgCl_2 \cdot 8H_2O$ formation. These additions cause a reduction in compressive strength and thermal stability, setting times increase due to delayed formation of hydration products and there is increased gel pores (<10 nm). These effects are caused by both additives but are most pronounced for MOC cement pastes containing phosphoric acid.

Keywords: magnesium oxychloride; phosphoric acid; tartaric acid; hydration; microstructure.

1. Introduction

Magnesium oxychloride (MOC) cements are formed by reacting reactive magnesia with magnesium chloride solution with compositions in the MgO-$MgCl_2$-H_2O ternary system [1-4]. They have high early strength, low density, low thermal conductivity and excellent fire resistance [5-6] and as a result are widely used as lightweight partition boards and in fireproof thermal insulation products, particularly in China. MOC cements are not toxic and they have been investigated as potential re-sorbable or thopaedic biomaterials [4]. They are also low-carbon cements because the temperature and energy needed to form light-burned magnesia (LBM) are much lower than required to manufacture Portland cement [7-8]. MOC cements can also be combined with coal fly ash and silica fume, to further improve environmental characteristics [9-12]. The major problem that limits more widespread use of MOC cements in construction is low water resistance [13].

The hydration products at room temperature of MOC cement pastes are $5Mg(OH)_2 \cdot MgCl_2 \cdot 8H_2O$ (phase 5) and $3Mg(OH)_2 \cdot MgCl_2 \cdot 8H_2O$ (phase 3) [3,14]. Phase 5 is the main binding phase that provides mechanical strength. The molar ratios of $MgO/MgCl_2$ and $H_2O/MgCl_2$ used to form MOC cements influences the composition of the hydration products [15]. These can be either phase 5 and phase 3, phase 5 and magnesium hydrate, or a mixture of phase 3, phase 5 and magnesium hydrate [3,15,16].

When MOC cement pastes are immersed in water, phase 5 and phase 3 decompose to $Mg(OH)_2$. The use of additives can influence this decomposition and ~4 wt.% additions of ferrous sulfate have been reported to improve the water resistance of MOC cements [17]. Incorporating complex water-resisting additives can also reduce the effect of water on magnesite material[18]. Soluble phosphates decrease the concentration of Mg^{2+} required for the formation of phase 5 in MOC cement and this enhances phase 5 stability in water [19]. Low levels of additives improve the water resistance of MOC cement by changing the microstructure and increasing phase 5 formation [3,19-21].

Previous research has used tartaric acid ($C_4H_6O_6$) and phosphoric acid (H_3PO_4) to improve the water resistance of MOC cement but understanding of how these change the hydration products, pore structure and performance of MOC cement is limited. The aim of this research was to investigate and understand the effect of tartaric acid (TA) and phosphoric acid (PA) additions on the compressive strength, thermal stability, composition, setting time, pore structure, microstructure and water resistance of MOC cement pastes.

2. Materials and methods

2.1 Materials

Light-burned magnesia (LBM) was produced by calcining magnesite ($MgCO_3$)obtained from Haicheng, in Liaoning Province China, at 800 ℃ for ~2 hours. The original magnesite had particles with diameters between 8 and 15 mm. After calcining the magnesia was crushed and sieved to produce a powder with particles < 0.074 mm. The LBM powder was analyzed by x-ray fluorescence (XRF, S8 Tiger, Bruker, Germany) and the resulting chemical composition data is given in Table 1.

Table 1
Chemical compositions of LBM

Components	Mass fraction (%)					
	MgO	CaO	SiO_2	Al_2O_3	Fe_2O_3	Others
LBM	89.13	2.34	1.41	0.42	0.47	6.23

2.2. Specimens preparation

The amount of reactive MgO present was determined by mixing 2.0 g of LBM powder with 20 mL of distilled water. The sample was cured at 20 ± 2 ℃ at a humidity of 65 ± 5 % for 24 hours and then heated to 105 ℃ for 24 hours. It was then further heated 150 ℃ until constant weight was achieved. The remaining solids sample was weighed and the content of reactive MgO (W) in the original LBM powder calculated from:

$$W = \frac{(W1-W0)}{0.45W0} \times 100\%$$

where W_0 is the original weight of the LBM powder (g); W_1 is the weight of LBM powder after hydration (g) and 0.45 is the molecular weight ratio between H_2O and MgO. This indicated that the content of active MgO in LBM was 65.50 wt% [22].

Magnesium chloride hexahydrate ($MgCl_2 \cdot 6H_2O$), phosphoric acid (PA) and tartaric acid (TA) were supplied as analytical grade chemicals (Ruijinte Chemical Co Ltd., Tianjin, China). PA and TA were added at 1 wt.% additions relative to the quantity of light-burned magnesia because preliminary work indicated that this was effective at improving the water resistance of MOC cements. N-MOC samples contained no additives, while TA-MOC contained 1 wt.% TA and PA-MOC contained 1 wt.% PA.

2.3 Test methods

Setting times were determined using the Vicat test at 20 ± 3 ℃ (GB/T 1346-2001). Compressive strengths of MOC cement pastes was determined with a 300 kN capacity universal testing machine using a loading rate of 2400 N/s[23].

After curing for 28 days, selected MOC cement paste samples were crushed and sieved to form a powder with particle size of < 70 μm. This was then subjected to thermal analysis (TG-DSC, STA 449F3, Netzsch) with samples heated from ambient to 650 ℃ at a heating rate of 10 ℃/min in a N_2 atmosphere.

X-ray diffraction (XRD, X Pert powder) was also used to analyze powder samples from 5 ° to 85° (2θ) using a step size of 0.0065° with 5 seconds per step. The Rietveld method with Topas5.0 software was used to complete quantitative analysis of the MOC cement paste samples[24-25]. Fourier Transform Infrared Spectroscopy (FTIR, Agilent Technologies Cary 630 FTIR) in the wave number range from 450 - 4000 cm^{-1} was also used to characterize hydrated MOC cement pastes.

Mercury intrusion porosimetry (MIP, AutoPoreIV9500) was used to determine the pore size distribution of MOC cement pastes cured in air for 28 days. The MOC cement samples were cut into small 5mm cube samples and dried in an oven at 60 ℃ for 1 day prior to MIP testing.

The water resistance of MOC cements was assessed by immersing 28-day cured samples in water for 7, 28, 56 and 90 days. After removing the samples they were surfaces dried and tested to failure in compression. The compressive strength retention coefficient, R_f, indicates the water resistance of the MOC cement pastes and this was calculated from:

$$R_f = R_x/R_0$$

where R_0 is the compressive strength of the MOC cement paste samples cured in air for 28 days and R_x is the compressive strength of the MOC samples after soaking in water for different days.

Fracture surfaces of MOC cement pastes tested before and after soaking in water were gold coated and examined using scanning electron microscopy with energy dispersive X-ray spectroscopy (SEM/EDS, ΣIGMA HD).

3. Results

3.1 Compressive strength of MOC cement

Compressive strength data for MOC cement pastes is shown in Fig. 1. Strength increased with curing time, with both initial and later strengths reduced by adding TA or PA as previously reported[3,9]. The average 28-day strengths of N-MOC, TA-MOC and PA-MOC were 108 MPa, 99 MPa and 87 MPa, respectively.

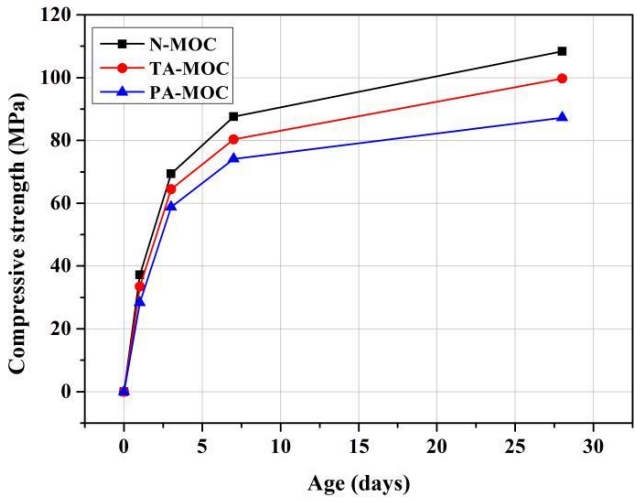

Fig. 1. Compressive strength of MOC cement with and without additives

3.2 Thermal analysis of MOC cement

Fig. 2 shows DSC data from thermal analysis for MOC cement pastes cured for 28 days. The DSC profiles of the different samples are very similar, showing five endothermic peaks determined by the compositions of the crystal phases formed. N-MOC has endothermic peaks at 137.3 ℃ 162.5 ℃ and 194.1 ℃ and these are attributed to thermal decomposition of $5Mg(OH)_2 \cdot MgCl_2 \cdot 8H_2O$ (phase 5) into $5Mg(OH)_2 \cdot MgCl_2$. Additional decomposition of $5Mg(OH)_2 \cdot MgCl_2$ into MgO occurs at higher temperatures and this produces endothermic peaks at 337.3 ℃ and 442.9 ℃ [26]. The addition of TA or PA shifts the endothermic peaks to lower temperatures and the endothermic peaks of PA-MOC are at lower temperatures than those of the TA-MOC samples.

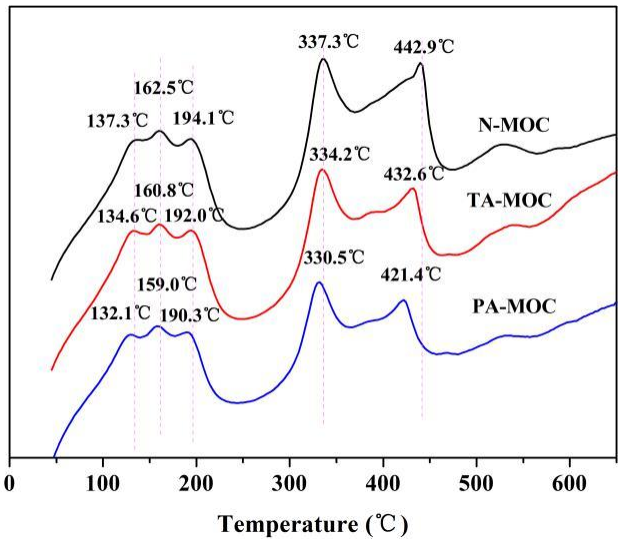

Fig. 2. DSC curves of MOC cement with and without additives at 28 days.

3.3 Phase composition

Fig. 3 shows XRD data for MOC cement pastes cured for 28 days. All samples contain significant amounts of phase 5, a small amount of $Mg(OH)_2$ and some residual MgO, $MgCO_3$ and SiO_2. Phase 5 and $Mg(OH)_2$ are hydration products while the other phases are present in the LBM. XRD data is summarized in Table 2 and this shows the mineralogical composition of MOC cement pastes is changed by the addition of TA and PA. TA and PA promote the formation of phase 5 and reduce formation of $Mg(OH)_2$. The content of phase 5 in N-MOC was ~ 58.3%. This increased to ~ 65.3% in TA-MOC and ~ 63.7% in PA-MOC.

The FTIR spectra in Fig. 4 show absorption bands at 3610.3 cm^{-1} and 3698.2 cm^{-1} which are attributed to stretching vibrations of OH in phase 5 and $Mg(OH)_2$. The peak intensity of N-MOC at 3610.3 cm^{-1} is lower than the peak at 3698.2 cm^{-1} indicating less phase 5 is present than $Mg(OH)_2$. From the peak intensities at 3610.3cm^{-1} and 3698.2 cm^{-1} it is apparent that less $Mg(OH)_2$ and more phase 5 is present in the MOC cement pastes containing TA and PA. The absorption band in the 3000-3600 cm^{-1} region is due to oxhydryl bond stretching vibration and the band between 1600 and 1640 cm^{-1} is attributed to H-O-H bending.

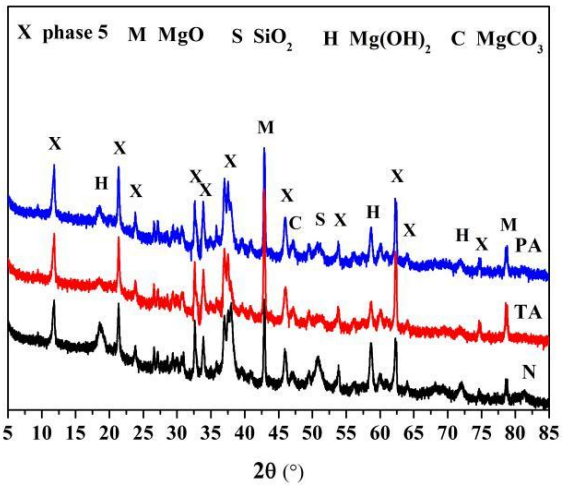

Fig. 3. X-ray patterns of MOC cement with and without additives at 28 days.

Table 2

Proportion of mineralogical composition in MOC cement at 28 days.

Sample	Mass fraction (%)					Rwp*
	Phase 5	MgO	$Mg(OH)_2$	$MgCO_3$	SiO_2	
N-MOC	58.32	19.02	14.26	7.68	0.72	10.686
TA-MOC	65.28	17.62	9.02	7.25	0.83	10.966
PA-MOC	63.74	20.12	7.87	7.61	0.66	11.012

*Rwp: R- weight pattern

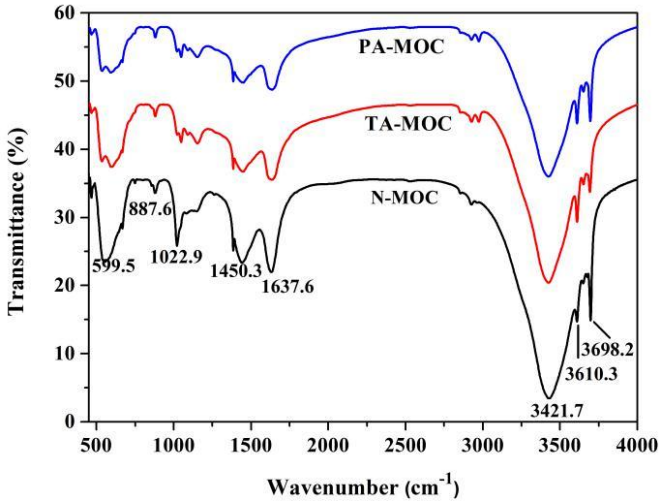

Fig. 4. FTIR spectra of MOC cement with and without additives at 28 days.

3.4 Microstructure of MOC cement

Fig. 5 shows fracture surfaces of MOC cement samples cured for 28 days. The hydration products form rod-like crystals in pores, while the bulk material consist of plate-like crystals. SEM/EDS analysis indicates that the hydration products are all phase 5. In addition, the plate-like crystals formed are interlocking in N-MOC (Fig. 5 (a)), while amorphous hydration products appear to be formed in TA-MOC and PA-MOC (Fig. 5 (b) and (c)).

The pore volume distribution data of the MOC cement pastes is given in Table 3 and Fig. 6 shows cumulative intruded volume vs pore diameter of MOC cement at 28 days. Small capillary pores (10-100 nm) and gel pores (<10 nm) are present. The amount of large pores (>100 nm), small capillary pores and gel pores in N-MOC were ~ 5.2%, ~ 71.9% and ~ 22.9%, respectively. The addition of TA and PA increased the volume of large pores and gel pores. However the volume of small capillary pores decreased compared to the N-MOC and the addition of TA and PA both results in a increase in total porosity.

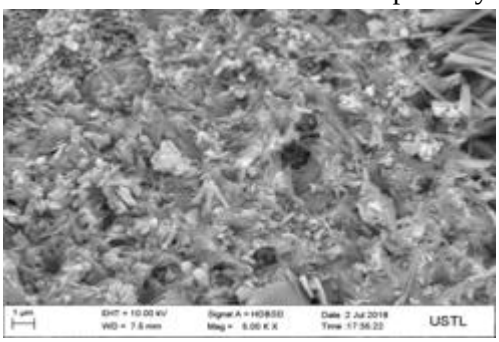

(a)

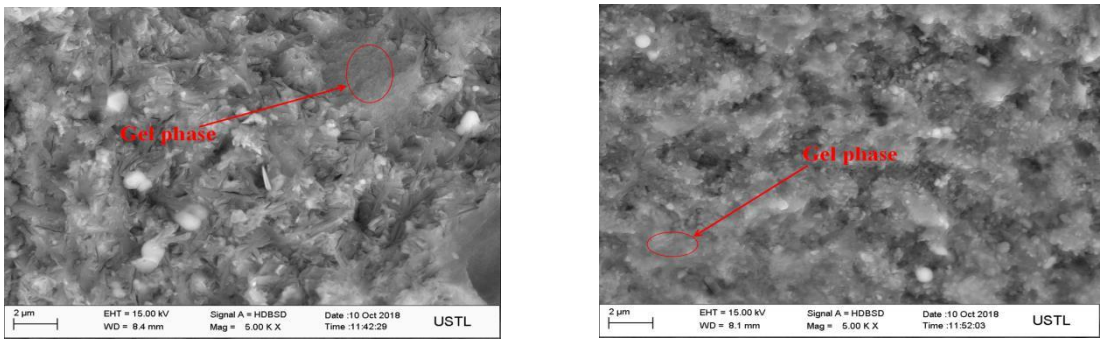

(b) (c)

Fig. 5. Microstructure of MOC cement with and without TA and PA at 28 days (a N-MOC, b TA-MOC, c PA-MOC).

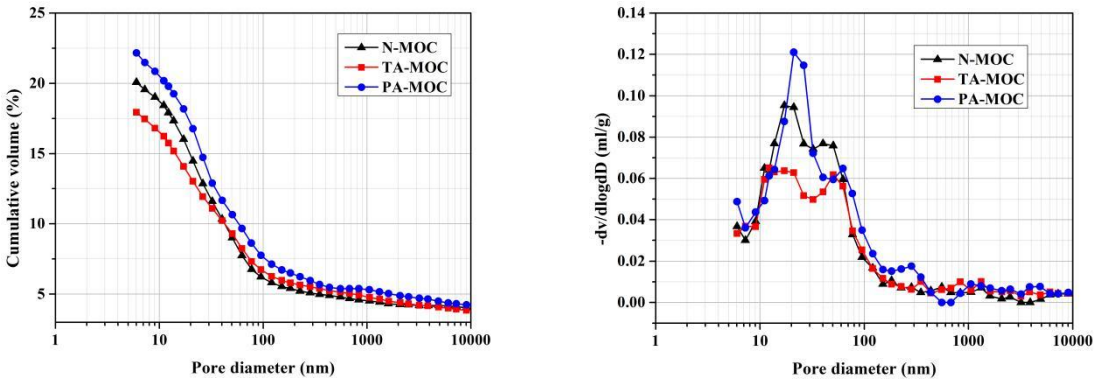

(a) (b)

Fig. 6. Cumulative intruded volume vs pore diameter of MOC cement at 28 days ((a) Cumulative intruded pore volume vs pore diameter, (b) Different intruded volume vs pore diameter)

Table 3

Pore distribution of MOC cement at 28 days.

Sample	Total intrusion volume (ml/g)	Total porosity (%)	Pore volume distribution (%)		
			> 100 nm	10-100 nm	< 10 nm
N-MOC	0.0990	17.94	5.21	71.86	22.93
TA-MOC	0.1121	20.06	5.88	66.56	27.56
PA-MOC	0.1256	22.16	6.03	69.62	24.35

3.5 Hydration of MOC cement

Fig. 7 shows Vicat setting data. The initial and final setting times increase for samples TA-MOC and PA-MOC compared to N-MOC. Fig. 8 shows XRD data for the MOC cement pastes during hydration at 3, 6, 8 and 16 hours. The rate of reaction of active magnesium oxide and magnesium chloride is rapid in N-MOC and after hydration for 6 hours extensive phase 5 has formed (Fig. 8 (a)). Addition of either TA or PA delays formation of phase 5. After 3 hours the main hydration product was $2Mg(OH)_2 \cdot MgCl_2 \cdot 2H_2O$ (phase 2·1·2)[4]. After 6 hours no phase 5 was detected (Fig. 8 (b) and (c)). After 8 hours, phase 2·1·2 had disappeared and phase 5 had formed, indicating phase 2·1·2 may transform into phase 5.

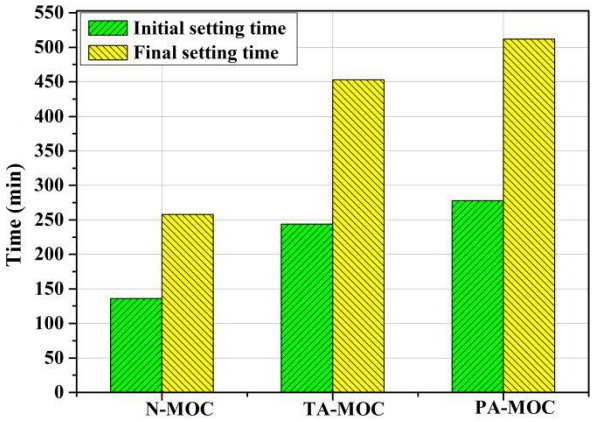

Fig. 7. Setting time of MOC cement with and without additives.

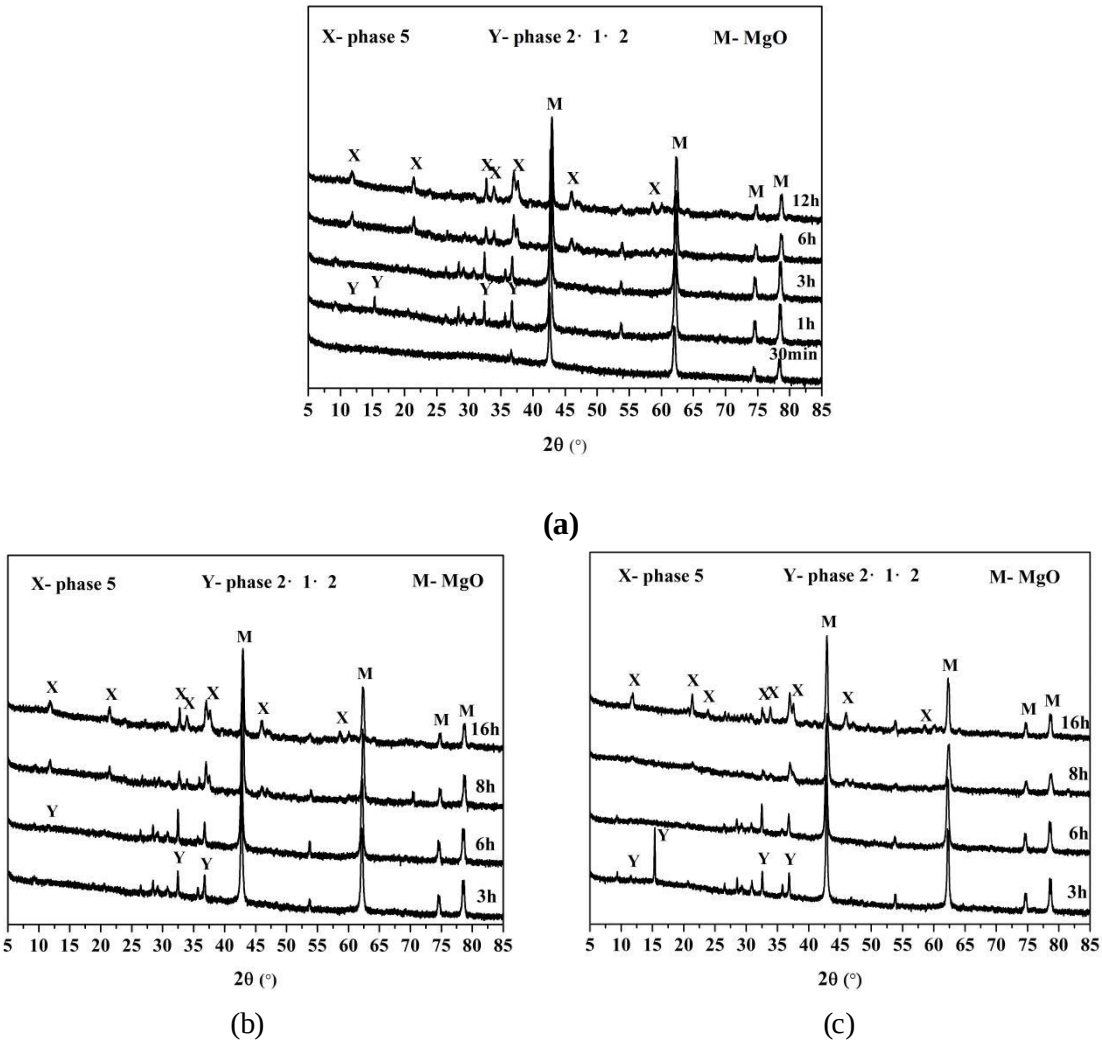

Fig. 8. XRD patterns of MOC cement with and without additives after hydration for various time (a N-MOC, b TA-MOC, c PA-MOC).

3.6. Water resistance of MOC cement

Fig. 9 shows the compressive strength data for MOC cement pastes after different immersion times in water. The water resistance of N-MOC is low and the compressive strength retention coefficients is 0.36 after soaking for 7 days and 0.16 after 28 days. At

longer soaking times the N-MOC samples begin to disintegrate. The addition of TA and PA markedly improve the water resistance of MOC cement pastes. Both TA-MOC and PA-MOC have much greater water resistance than N-MOC with PA appearing to be marginally more effective than TA.

Fig. 10 shows XRD patterns of MOC cement pastes after soaking in water for 28 days. Phase 5, $Mg(OH)_2$, $MgCO_3$, SiO_2 and MgO were present in MOC cement pastes. After soaking in water for 28 days the peak intensities of phase 5 and MgO decreased and increased for $Mg(OH)_2$. Results are summarized in Table 4. The main hydration product in MOC cement with additives was phase 5 and this did not decrease after soaking in water. The main hydration product in N-MOC was $Mg(OH)_2$ with much less phase 5. Both TA and PA enhance the stability of phase 5 in water and do not impede hydration of unreacted MgO in water.

Fig. 11 shows the microstructure of the MOC cement pastes after soaking in water for 28 days. There appears to be reduced phase 5 present in N-MOC samples. In addition, the amount of porosity compared to the microstructure of N-MOC at 28 days has significantly increased. This is believed to be due to loss of phase 5 and formation of $Mg(OH)_2$ as a result of water immersion.

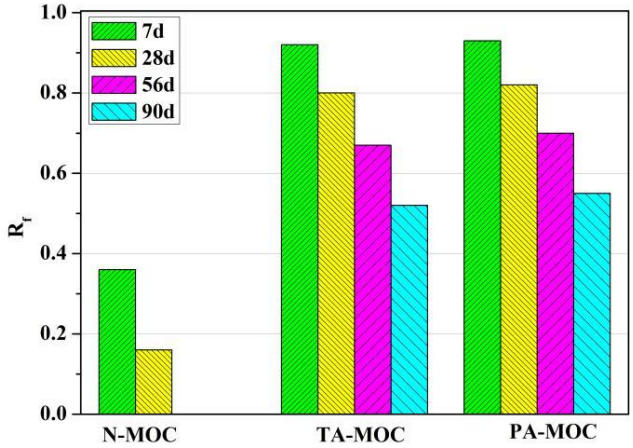

Fig. 9. Compressive strength retention coefficient of MOC cement with and without additives.

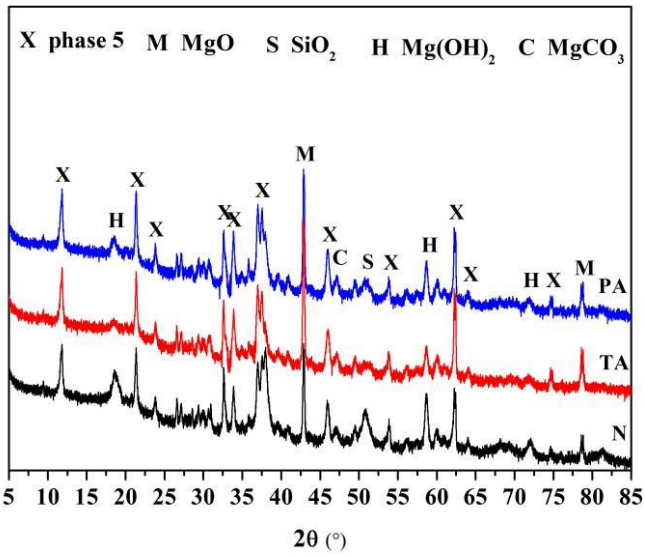

Fig. 10. X-ray patterns of MOC cement with and without additives after soaking in water

Table 4

Proportion of mineralogical composition in MOC cement after soaking in water for 28 days.

Sample	Mass fraction (%)					Rwp*
	Phase 5	MgO	$Mg(OH)_2$	$MgCO_3$	SiO_2	
N-MOC	23.76	10.64	56.95	7.96	0.69	10.546
TA-MOC	57.88	9.03	24.56	7.73	0.80	10.735
PA-MOC	55.29	12.42	23.80	7.85	0.64	11.414

*Rwp: R- weight pattern

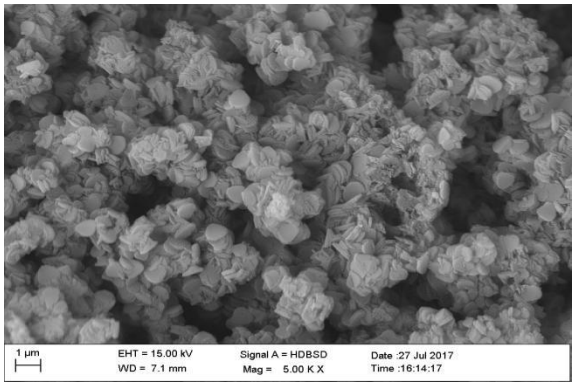

(a)

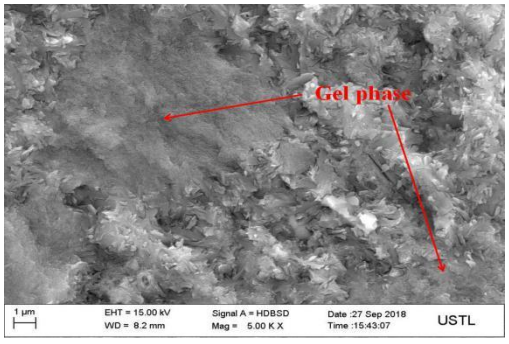

(b)

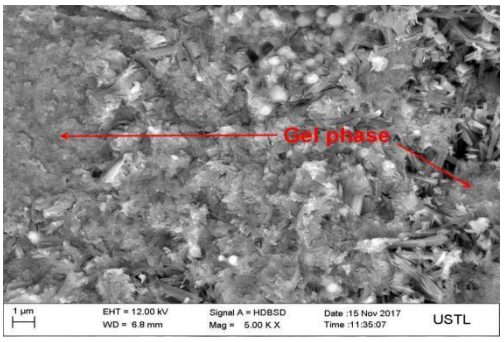

(c)

Fig. 11. The microstructure of MOC cement with and without additives after soaking in water for 28 days (a N-MOC, b TA-MOC, c PA-MOC).

Discussion

The XRD data and FTIR data show that TA and PA reduce the amount of $Mg(OH)_2$ formed during hydration of MOC cement. This is because when MgO is mixed with $MgCl_2$ solution, OH^- and $[Mg(OH)(H_2O)_x]^+$ form on the surface of the MgO (Eq. (1))[27] and $[Mg(OH)(H_2O)_x]^+$ reacts further with OH^- in solution (Eq. (2))[28]. However, $[Mg(OH)(H_2O)_x]^+$ may combine with acid group ions if TA or PA are in the solution. This results in the growth of $[TA^{n-} \rightarrow Mg(OH)(H_2O)_{x-1}]$ and $[H_2PO_4 \rightarrow Mg]^+$ on the surface of MgO as shown in Eq. (3) and (4)[27-29]. The formation of hydration shells on the surface of MgO is believed to limit formation of additional $Mg(OH)_2$:

$$MgO + (x+1)H_2O \rightarrow [Mg(OH)(H_2O)_x]^+_{(surface)} + OH^- \quad (1)$$

$$[Mg(OH)(H_2O)_x]^+_{(surface)} + OH^- \rightarrow Mg(OH)_2 \quad (2)$$

$$TA^{n-} + [Mg(OH)(H_2O)_x]^+_{(surface)} \rightarrow [TA^{n-} \rightarrow Mg(OH)(H_2O)_{x-1}]_{(surface)} + H_2O \quad (3)$$

$$H_2PO_4^- + Mg^{2+} \rightarrow [H_2PO_4 \rightarrow Mg]^+_{(surface)} \quad (4)$$

The lattice energy of gel phase 5 is low due to poor crystallinity and this causes thermal

decomposition at lower temperatures as shown in Fig. 2[30]. The acid groups of TA or PA are absorbed on the surface of phase 5 and form Mg-O-CO-R or Mg-O-$PO(OH)_2$ coordination bond[20,29], and these weaken adjacent Mg-Cl and Mg-O bonds of phase 5, reducing thermal stability. The DSC results show that the decomposition temperature is in the order N-MOC> TA-MOC> PA-MOC.

The increase of gel pores and decrease of capillary pores in MOC containing either TA or PA indicates increased formation of gel phase. The acid groups of TA and PA cause the transformation of phase 5 into a gel phase which can fill small capillary pores. Adding PA and TA also formed more gel phase 5 and less $Mg(OH)_2$ (Table 2) which may cause the proportion of gel pores to increase and small capillary pores to decrease. The increase in large pores in MOC cement with TA and PA may be due to the formation of CO_2 from the reaction of H^+ and $MgCO_3$ in the slurry. The total porosity in TA-MOC and PA-MOC are similar to other data in the literature[3]. The increasing total porosity in PA-MOC and TA-MOC decreases the compressive strength of paste samples compared to N-MOC.

The addition of TA and PA delay the formation of hydration products. The acid group ions of TA and PA can adsorb on the surface of MgO particles to form $[TA \rightarrow Mg(OH)(H_2O)_{x-1}]$ and $[H_2PO_4 \rightarrow Mg]^+$ and this forms a hydration shell which restricts further the hydration of MgO particles (Eq. (3) and (4)). The acid group ions of TA and PA also forms coordination bonds with Mg^{2+} in phase 5 which delays the hydration and setting of MOC cement. Although TA and PA delay hydration, the hydration products are similar. XRD data shows that phase 2 ·1 ·2 is formed in the early stages of hydration, and as the hydration increases, phase 2 ·1 ·2 disappearsand phase 5 is formed. The formation of phase 2 ·1 ·2 is given by Eq. (5), while with the incorporation of TA and PA is explained by Eq. (6) and (7). In addition, the observation the transformation of phase 2 ·1 ·2 into phase 5 is given by Eq. (8).

$$2[Mg(OH)(H_2O)_x]^+_{(surface)} + [Mg(OH)(H_2O)_x]^+_{(aq)} + 2Cl^- + OH^- \rightarrow$$
$$2Mg(OH)_2 \cdot MgCl_2 \cdot 2H_2O + (2x-2)H_2O \quad (5)$$

$$2[TA^{n-} \rightarrow Mg(OH)(H_2O)_{x-1}]_{(surface)} + [Mg(OH)(H_2O)_x]^+_{(surface)} + 2Cl^- + OH^- \rightarrow$$
$$2Mg(OH)_2 \cdot MgCl_2 \cdot 2H_2O + (2x-3)H_2O + 2TA^{n-} \quad (6)$$

$$[H_2PO_4 \rightarrow Mg]^+_{(surface)} + 2[Mg(OH)(H_2O)_x]^+_{(surface)} + 2Cl^- + 4OH^- \rightarrow$$
$$2Mg(OH)_2 \cdot MgCl_2 \cdot 2H_2O + (2x+2)H_2O + 2PO_4^{3-} \quad (7)$$

$$2Mg(OH)_2 \cdot MgCl_2 \cdot 2H_2O + 3[Mg(OH)(H_2O)_x]^+_{(surface)} + 3OH^- \rightarrow$$
$$5Mg(OH)_2 \cdot MgCl_2 \cdot 8H_2O + (3x-6)H_2O \quad (8)$$

When MOC cement pastes are immersed in water the crystal structure of phase 5 is effected by the loss of Mg^{2+} and Cl^-, and finally translate into $Mg(OH)_2$ (Eq. (9)). The plate-like phase 5 crystals transform into a gel phase 5 rather than $Mg(OH)_2$ in TA-MOC and PA-MOC, indicating that adding TA or PA improves the stability of phase 5. In addition, the reduced volume proportion of gel pores (< 100 nm) may also improve the water resistance of TA-MOC and PA-MOC[3]. However, as shown in Fig. 9, as the soaking time increases, the compressive strength retention coefficients of TA-MOC and PA-MOC gradually decrease. This indicates that although adding TA or PA can improve the stability of MOC cement pastes in water, decomposition of phase 5 cannot be completely inhibited.

$$5Mg(OH)_2 \cdot MgCl_2 \cdot 8H_2O_{(s)} + nH_2O \rightarrow 5Mg(OH)_{2(s)} + 2Cl^-_{(aq)} + Mg^{2+}_{(aq)} + (n+8)H_2O \quad (9)$$

Conclusions

The addition of 1 wt.% of tartaric acid (TA) or phosphoric acid (PA) to MOC cements

significantly improves water resistance of paste samples. This is associated with increased $5Mg(OH)_2 \cdot MgCl_2 \cdot 8H_2O$ (phase 5) formation with reduced crystallinity due to coordination effects between the acid group of TA and PA and Mg^{2+} ions. The additives reduce compressive strength and setting times increase and these effects are most pronounced for MOC cement pastes containing PA. The increased setting time and reduced strength result from reduced hydration of MgO due to increased stability of hydration shells that inhibit formation of $Mg(OH)_2$. TA and PA additions increase total porosity by increasing the volume of large pores (>100 nm) and fine gel pores (<10 nm). Immersing TA-MOC and PA-MOC in water for 28 days causes the plate-like phase 5 to transforms into a gel form of phase 5 and this is believed to contribute to improved water resistance. The addition of TA or PA to MOC does improve the water resistance but decomposition of phase 5 is not completely inhibited.

Acknowledgements

The financial support of this work was supported by the National Science Foundation of China (No.51772139, 51778101), National Key R&D Program of China (2017YFE0107000) and Dalian High-level Talent Innovation Program (2017RQ051).

5. References

[1] Z.J. Li, C.K. Chau, Influence of molar ratios on properties of magnesium oxychloride cement, Cem. Concr. Res. 37 (6) (2007) 866-870.

[2] T. Demediuk, W.F. Cole, H.V. Hueber, Studies on magnesium and calcium oxychlorides, Aust. J. Chem. 8 (2) (1955) 215-233.

[3] Y. Li, Z.J. Li, H.F. Pei, H.F, Yu. The influence of $FeSO_4$ and KH_2PO_4 on the performance of magnesium oxychloride cement, Constr. Build. Mater, 102 (2016) 233-238.

[4] Y.N. Tan, Y. Liu, L. Grover, Effect of Tartaric acid on the properties of magnesium oxychloride cement as a biomaterial, Cem. Concr. Res. 56 (2) (2014) 69-74.

[5] Z.Y. Lu, J.R. Zhang, G.X. Sun, B.W. Xu, Z.J. Li, C.C. Gong, Effects of the form-stable expanded perlite/paraffin composite on cement manufactured by extrusion technique, Energy 82 (2015) 43-53.

[6] B.W. Xu, H.Y. Ma, C.L. Hu, Z.J. Li, Influence of cenospheres on properties of magnesium oxychloride cement-based composites, Mater. Struct. (2015) 1-8.

[7] Y. Guan, W.L. Bi, L. Zhang, Experiment of the preparation of activated MgO by calcining low grade magnesite. Energy for Metallurgical Industry, 2015 (in Chinese).

[8] X.W. Liu, Y.L. Feng, H.R. Li, P. Zhang, P. Wang, Preparation of light-burned magnesia from magnesite and its hydration kinetics, J. Cent. South Univ. 42 (12) (2011) 3912-3917.

[9] H.F. Yu, S.T. Li, Q.Y. He, X.Q. Ding, Research on long term strength and water resistance of MgO–SF–FA–$MgCl_2$–H_2O system cementitious materials, J. Chin. Ceram. Soc. 28 (S1) (2000) 33-37 (in Chinese).

[10] Y. Li, H. Yu, L. Zheng, J. Wen, C. Wu, Y. Tan, Compressive strength of fly ash magnesium oxychloride cement containing granite wastes, Constr. Build. Mater. 38 (2013) 1-7.

[11] C.Y. Wu, H.F. Zhang, H.F. Yu, The effects of alumina-leached coal fly ash residue on magnesium oxychloride cement, Adv. Cem. Res. 25 (5) (2013) 254-261.

[12] C.K. Chau, J. Chan, Z.J. Li, Influence of fly ash on magnesium oxychloride mortar, Cem.

Concr. Com. 31 (2009) 250-254.
[13] Z. Zhou, H. Chen, Z. Li, H. Li, Simulation of the properties of MgO–$MgCl_2$–H_2O system by thermodynamic method, Cem. Concr. Res. 68 (2015) 105-111.
[14] D.H. Deng, C.M. Zhang, The formation mechanism of the hydrate phases in magnesium oxychloride cement, Cem. Concr. Res. 29 (9) (1999) 1365-1371.
[15] Y. Li, H.F. Yu, J.M. Dong, J. Wen, Y.S. Tan, Research development on hydration product, phase transformation and water resistance evaluation method of magnesium oxychloride cement, J. Chin. Ceram. Soc. 41 (11) (2013) 1465-1473 (in Chinese).
[16] W.F. Cole, T. Demediuk, X-ray, thermal and dehydration studies on magnesium oxychloride, Australian Journal of Chemistry. 8 (1955) 234-237.
[17] R.Weng, N. Liu, X.Y. Liu, X.L. Yang, Study of water resistance of magnesium oxychloride cement reinforced by glass fiber, Acta Mater, Compos, Sin. 15 (4) (1998) 30-34 (in Chinese).
[18] K.J. Xu, J.T. Tao, Y.Q. Guo, S.H. Dong, Effects of a new modifier on the water-resistance of magnesite cement tiles, Sol, Sta, Sciences. 14 (2012) 10-14.
[19] D.H. Deng, The mechanism for soluble phosphates to improve the water resistance of magnesium oxychloride cement, Cem, Concr, Res. 33 (9) (2003) 1311-1317.
[20] J. Wen, H.F. Yu, Y. Li, C.Y. Wu, J.M. Dong, L.N. Zheng, Effects of H_3PO_4 and $Ca(H_2PO_4)_2$ on mechanical properties and water resistance of thermally decomposed magnesium oxychloride cement, J. Cent. South Univ. 20 (12) (2013) 3729-3735.
[21] J. Wen, H.F. Yu, Y. Li, C.Y. Wu, J.M. Dong, L.N. Zheng, phosphoric acid on hydration process and of thermal decomposed magnesium oxychloride cement[J], Wuhan Univ, Sci, Technol, I. 29 (1) (2014) 114-118.
[22] J.M. Dong, H.F. Yu, L.M. Zhang, Study on experimental conditions of hydration methods of determining active magnesium oxide content, Int. J. Salt Lake Res. 18 (1) (2010) 38-41.
[23] ASTM C109/C109M, Standard Test Method for Compressive Strength of Hydraulic Cement Mortars (Using 2-in. or [50-mm] Cube Specimen.
[24] Y.S. Tan, H.F. Yu, Y. Li, W.L. Bi, X. Y. The effect of slag on the properties of magnesium potassium phosphate, Constr. Build. Mater. 126 (2016) 313-320.
[25] A.F. Gualtieri, Accuracy of XRPD QTA using the combined Rietveld-RIR method, J. Appl. Crystallogr. 33 (2) (2000) 267-278.
[26] R.E. Dinnebier, I. Halasz, D. Freyer, J.C. Hanson, The crystal structures of two anhydrous magnesium hydroxychloride phases from in situ synchrotron powder diffraction data, Z. Anorg. Allg. Chem. 637 (11) (2011) 1458-1462.
[27] C.Y. Wu, W.H. Chen, H.F. Zhang, H.F. Yu, The hydration mechaninsm and performance of modified magnesium oxysulfate cement by tartaric acid, Constr. Build. Mater. 144 (2017) 516-524.
[28] C.Y. Wu, H.F. Yu, J.M. Dong, L.N. Zheng, Effects of Material Ration, Fly Ash, and phosphoric acid on Magnesium Oxysulfate Cement, ACI Mater, J. 111 (3) 2014 291-297.
[29] N. Wang, H.F. Yu, W.L. Bi, Y.S. Tan, N. Zhang, C.Y. Wu, H.Y. Ma, S. Hua, Effects of sodium citrate and phosphoric acid on the properties of magnesium oxysulfate cement, Constr. Build. Mater, 169 (2018) 697-704.
[30] R.H.R. Castro, R.B. Torres, G.J. Pereira, D. Gouvea, Interface energy measurement of

MgO and ZnO: understanding the thermodynamic stability of nanocarticles, Chem. Mater. 22 (8) (2010) 2502-2509.